SUPPLEMENTARY INFORMATION

Yeast Mitochondrial RNAP Conformational Changes are Regulated by Interactions with the Mitochondrial Transcription Factor

Srdja Drakulic, Liping Wang, Jorge Cuéllar, David Guo, Gilberto Velasquez, Jaime Martín-Benito, Rui Sousa, José M. Valpuesta

INVENTORY OF SUPPLEMENTORY INFORAMTION:

Supplemental Figure S1: related to Figures 1 and 5

Supplemental Figure S2: related to Figures 1-3, and 5

Supplemental Figure S3: related to Figures 1 and 3

Supplemental Figure S4: related to Figures 2 and 4

Supplemental Figure S5: not related to any figure from the main text

Supplemental Figure S6: related to Figure 5

Supplemental Figure S7: not related to any figure from the main text

Supplemental references

A

```
                                  +1
5´(Non-template)-CGCGATATGCAGCTTAAAGAATAGTTTTA
    3´(Template)-GCGCTATATTCATTATTTCTTATCAAAAT
```

B

```
                                                          +1
5´(Non-template)-AATTCATTTATTTATTATTATATGCAGCTTAAAGAATAGTTTTATATACTAATAATAATATAG
    3´(Template)-TTAAGTAAATAAATAATAATATATTCATTATTTCTTATCAAAATATATGATTATTATTATATC
```

C

```
        5'(RNA)-GGAGGAAGAC
5'(Non-template)-ACACGTTACGTTCGCCACGGC
    3'(Template)-CCTCCTTCTGTACGCGTCCCG
```

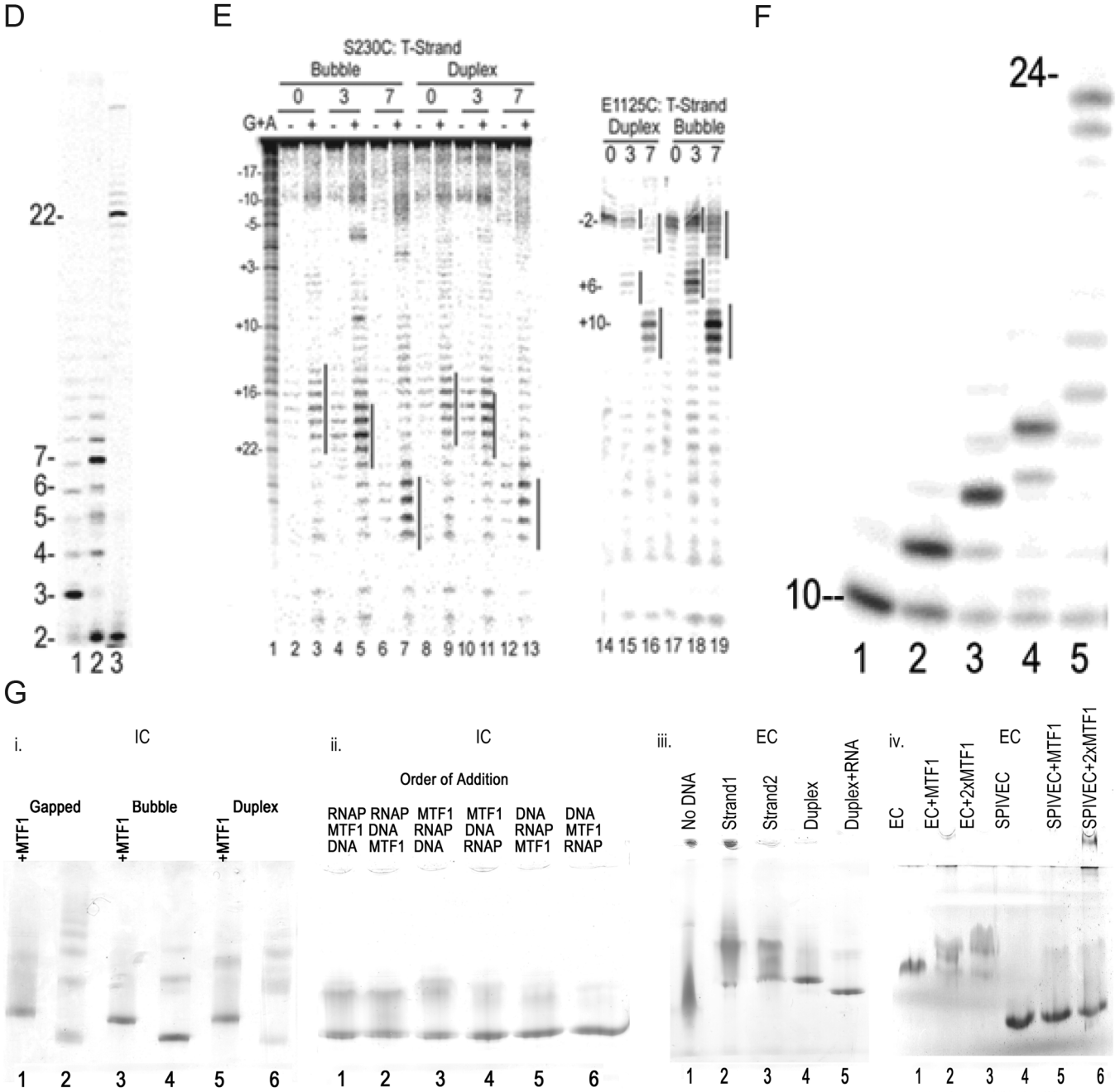

Figure S1 (related to Figsures 1 and 5). Synthetic promoters and DNA/RNA scaffolds used in these studies allow formation of physiologically relevant IC and EC structures. (A) Heteroduplex promoter used in the EM studies of the quasi-IC and IC ('bubble promoter'; 'IC DNA'). The promoter region from -8 to +2 corresponds to the sequence of the yeast mitochondrial 14s rRNA promoter (1). The underlined and italicized region is the segment of the NT whose sequence was altered to create a promoter in which the -4 to +2 region is effectively pre-melted. In the fully duplex version of this promoter the NT-strand is fully complementary to the T-strand. **(B)** Heteroduplex promoter used in the experiments with Fe-BABE conjugated MTF1 and MtRNAP, and in the transcription reactions to assess mutant activity The underlined and italicized region is the segment of the NT

strand whose sequence was altered to create a promoter in which the -4 to +2 region is effectively pre-melted. In the fully duplex version of this promoter the NT-strand is fully complementary to the T-strand. **(C)** EC RNA/DNA scaffold ('EC DNA') used in the EM studies of the EC. Nucleotides of 21 base pairs long DNA and 10 nucleotides long RNA that form transcription bubble are underlined and italicized. **(D)** Transcription in the presence of limiting NTPs/3'-dNTPs halts transcription at defined transcript lengths. Lane 1: Transcription in the presence of ATP and 3'-dUTP limits transcript extension to 3mer length. Lane 2: Transcription with ATP, UTP, and 3'-dGTP halts transcription at 7mer. Lane 3: Transcription with ATP, UTP, GTP, and 3'-dCTP. All reactions contained α^{32}P-ATP for transcript labeling and 14s bubble promoter template, MtRNAP, and MTF1 at 0.2, 0.4, and 0.8 μM, respectively. **(E)** ICs formed on duplex and pre-melted ('bubble') promoter templates are structurally and functionally similar. Lane 1 shows markers (G+A) lanes for mapping the positions of cleavage patterns on the template ("T") strand in either bubble or duplex promoters, as indicated. Cleavage of the DNA strands was initiated by adding ascorbate and peroxide to transcription complexes formed with MTF1 in which S230 was mutated to cysteine (S230C) and then conjugated with Fe-BABE (2) (lanes 2-13), or with mtRNAP in which E1125 was mutated to cysteine and similarly conjugated (lanes 14-19). Lanes labeled "-" did not have ascorbate and peroxidase added to activate the nuclease; lanes labeled "+" show reactions to which ascorbate and peroxidase were added. Lanes 14-19 show only reactions to which ascorbate and peroxidase were added. Reactions also contained NTPs allowing RNA extension to 0 (no NTPs), 3 (ATP+3'dUTP), or 7 nts (ATP+UTP+3'dGTP), as indicated. The cutting patterns on the duplex and bubble promoters are very similar in position and shift downstream identically in response to addition of NTPs. **(F)** ECs were formed with mtRNAP, partially heteroduplex T and NT strands, and a 10 nt RNA labeled with ^{32}P at its 5'end. They were then incubated in transcription buffer with no NTPs (lane 1), 3'dATP (lane 2), ATP+3'dUTP (lane 3), ATP+UTP+3'dCTP (lane 4) or all 4 NTPS (lanes 5). In reactions with NTPs most of the 10 base RNA is extended to the length expected for template directed transcription. **(G)** NATIVE PAGE analysis of complexes used in these studies. i. Complexes formed with 29 bp promoters in which the region around the transcription start site was heteroduplex as in 'B' ('Bubble'; lanes 3,4), or in which the promoters were fully duplex ('Duplex'; lanes 5, 6) or missing the -4 to +2 region of the NT strand ('Gapped'; lanes 1, 2). All reactions contained mtRNAP and no (even lanes) or equimolar amounts of MTF1 (odd lanes). The most homogeneous complexes were obtained with duplex or bubble promoters in the presence of MTF1 and with bubble promoters without MTF1 and were used in subsequent experiments. ii.Order of addition experiments were carried out to determine the best way to form ICs. The most homogeneous complexes were obtained by adding MTF1 to promoter DNAs followed by mtRNAP. iii. Formation of complexes with different EC nucleic acid components. Lane 1: mtRNAP alone runs as a smear and is partially retained as an aggregate at the point of loading. Lanes 2 and 3: Addition of a single DNA strand from the heteroduplex construct shown in C results in complexes that run as smears. Lane 4: mtRNAP with annealed heteroduplex runs as single band with some slower migrating species presnet. Lane 5: mtRNAP with annealed heteroduplex and RNA (as in C) runs as single species suitable for EM analysis. iv. Artificial ECs show approriate weak binding to MTF1. ECs formed with full-length mtRNAP (lanes 1-3) or SPIVRNAP (missing residues 1-240; lanes 4-6) were run in the presence of no (lanes 1, 4), 1:1 (lanes 2, 5), or 2:1 excess MTF1 (lanes 3, 6). Relative to ICs, which supershift fully upon addition of 1:1 MTF1, the ECs exhibit reduced MTF1 binding as evidenced by incomplete and smeared supershifted species with full-length mtRNAP (lanes 2,3) and neglible supershifts with SPIVRNAP (lanes 5, 6), reflecting weaker MTF1 binding by the latter.

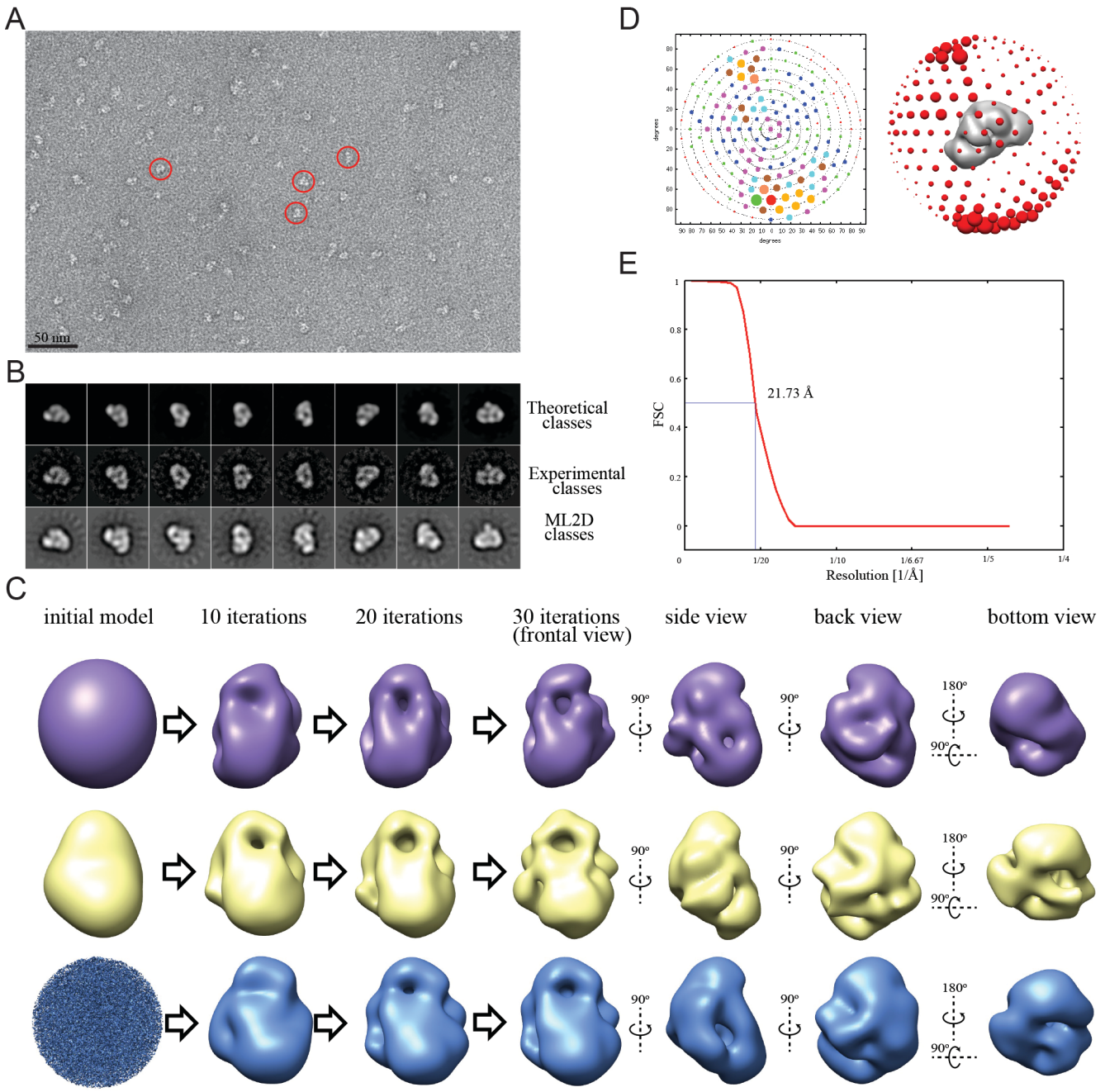

Figure S2 (related to Figures 1-3, and 5). A scheme of the 3D reconstruction procedure. (A) An example of a typical negative staining micrograph of the IC complex, with some selected individual particles (red circles). **(B)** The quality of 3D reconstruction is represented at the example of the IC, where further validation can be obtained by comparison of final 3D map projections and generated class averages (EMAN) with the results of ML2D classification. **(C)** The different processing steps in EMAN starting from 3 different initial models: blob (purple), common lines (yellow) and noise (blue) are shown for IC. The need for independent reconstructions is the consequence of a model bias that is present in all existing program packages. Thus, they represent a validation mechanism for the model that will be submitted to the final steps of processing in XMIPP. **(D)** 2D and 3D representation of angular distribution of the particles that were used in the final step of 3D reconstruction of IC, performed by Projection Matching. Each circle (2D) or sphere (3D) represents one projection of the final model with defined angular values. Their size is proportional to the number of assigned individual particles. **(E)** The computed resolution curve of IC. The resolution of the obtained model has been estimated to be 21.7 Å with the 0.5 criterion.

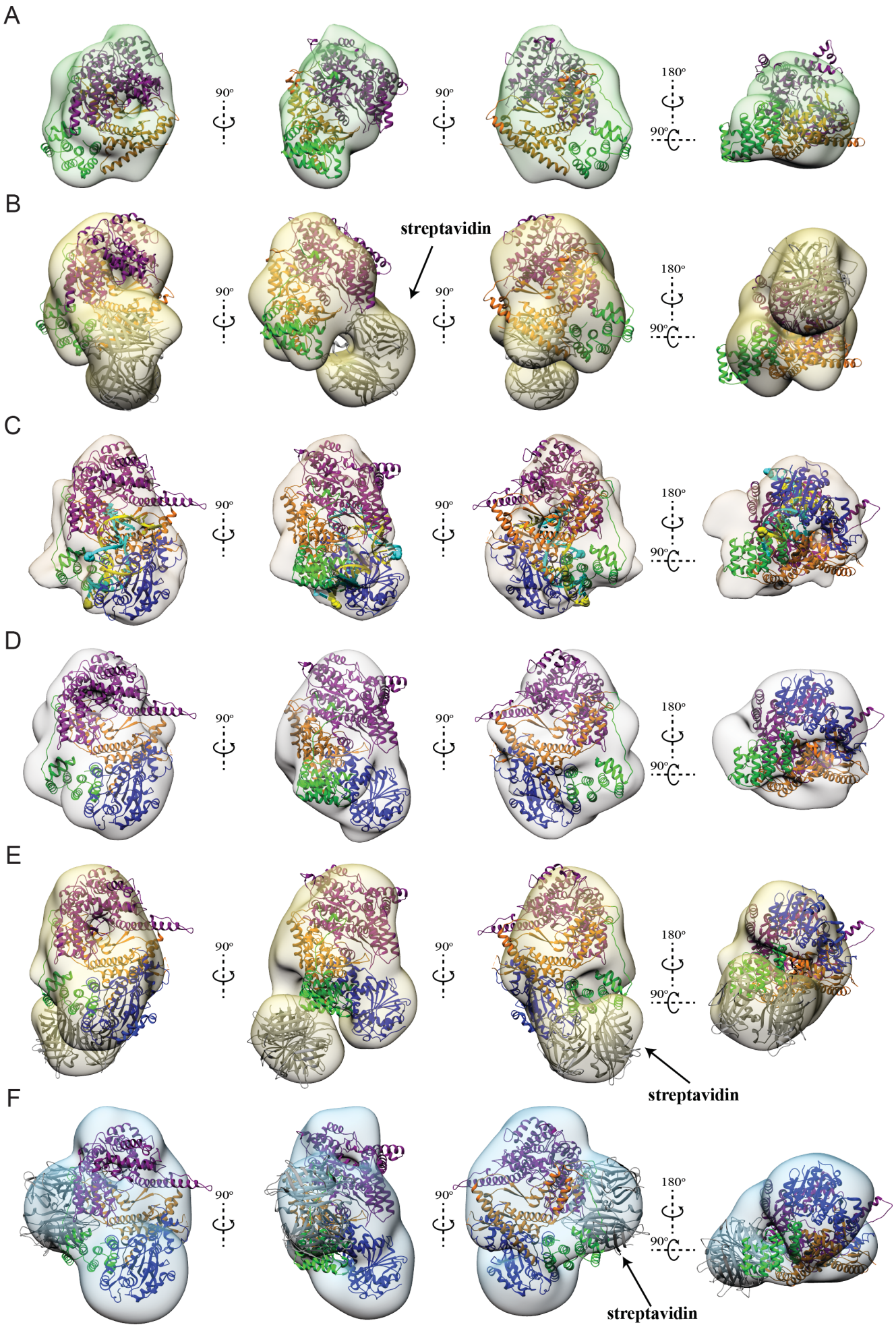

Figure S3 (related to Figures 1-3). 3D reconstructions of the quasi-ICs and ICs. The same views of the 3D reconstructions (together with the docking of the crystal structure of human mtRNAP (pdb 3SPA; in the case of quasi

and biotin labeled quasi-IC), of MTF1 (pdb 1I4W) and of the atomic structure of human MtRNAPEC (pdb 4BOC; ICs; DNA has not been shown). **(A)** Quasi-IC (12848 particles; 19 Å resolution). **(B)** quasi-iC in which the 5'-end of the NT-strand DNA is labeled with biotin/streptavidin ('upstream streptavidin quasi-IC') (16514 particles; 18 Å resolution). **(C)** IC from unstained, frozen-hydrated particles (10893 particles; 15 Å resolution). The DNA of aligned atomic structure of T7RNAPIC at 7nts long step (pdb 3E2E) has been shown. T and NT strands have been colored in cyan and yellow, respectively, with their 5´ ends emphasized by spheres **(D)** IC from negatively-stained particles (15917 particles; 22 Å resolution). **(E)** IC which the 5'-end of the NT-strand DNA is labeled with biotin/streptavidin ('upstream streptavidin IC') (21662 particles; 17 Å resolution). **(F)** IC in which the 5'-end of the T-strand DNA is labeled with biotin/streptavidin ('downstream streptavidin IC') (21200 particles; 18 Å resolution).

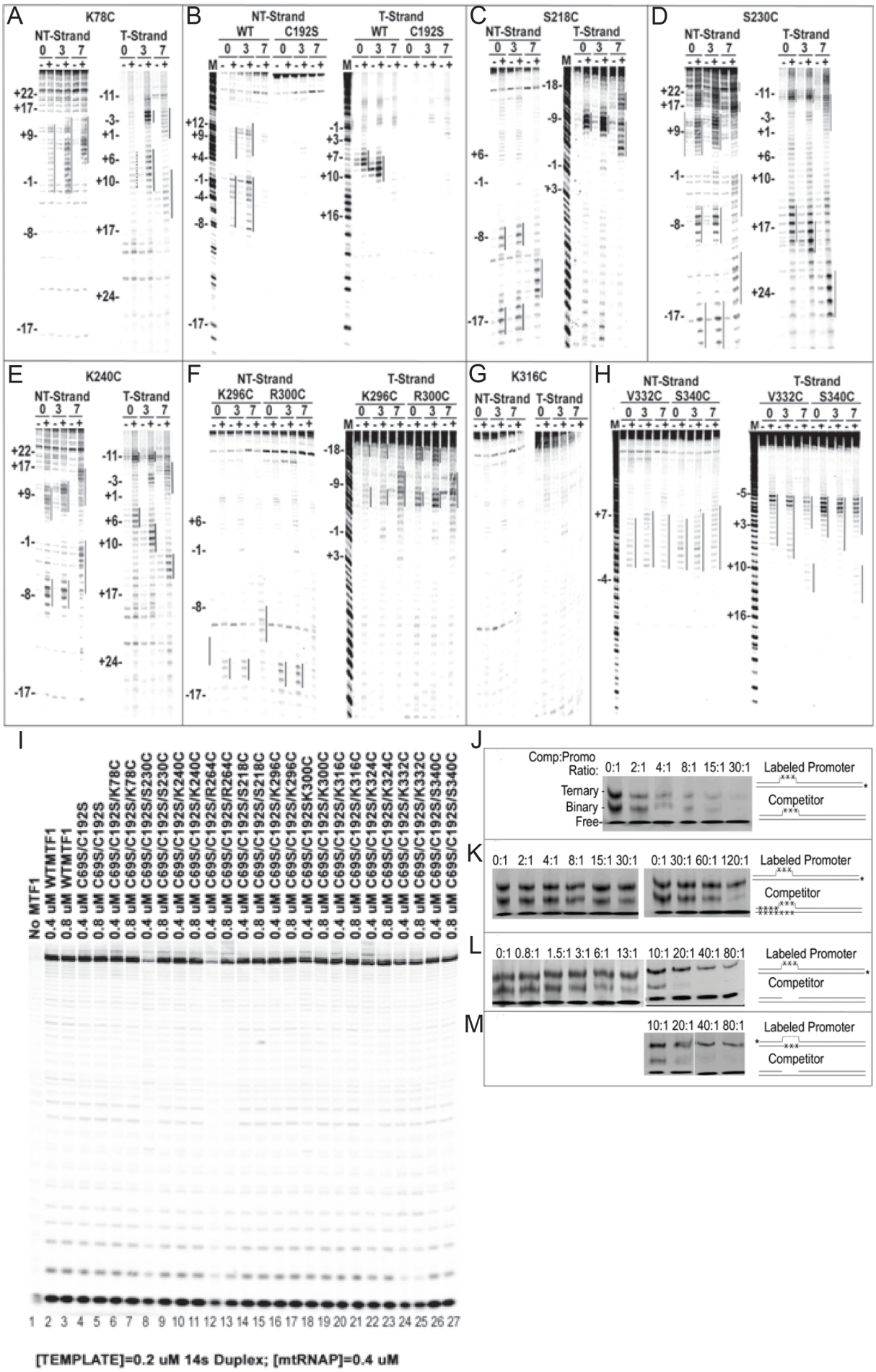

Figure S4 (related to Figures 2 and 4). The MTF1´s role and position in IC. (A-H) DNA cutting patterns of chemical nucleases conjugated to different sites on MTF1 confirm and refine the IC model

developed from EM data. Each panel shows the cleavages on either the NT- or T-strands, as indicated, in reactions with mtRNAP and the indicated mutant MTF1 molecules conjugated with Fe-BABE. "M"=G+A markers used to map the cleavage sites with respect to the +1 transcription start site; "-" and "+" refer, respectively, to absence or addition of ascrobate/peroxide to activate cleavage (low levels of cutting are seen even in the absence of a ascorbate/peroxide). NTPs allowing RNA extension to 0 (no NTPS), 3 (ATP+3'-dUTP), or 7 (ATP+UTP+3'-dCTP) nts, as indicated were added to the reactions. **(I)** MTF1 mutants support transcription on duplex templates (the yeast mitochondrial 14s rRNA promoter sequence, see Figure S1B) at levels similar to WT MTF1. Transcription reactions carried out with duplex templates at 0.2 μM and MtRNAP at 0.4 μM and with no MTF1 (lane 1) or WT or indicated mutants MTF1 at 0.4 or 0.8 μM MtRNAP, as indicated. In the absence of MTF1 there is little transcription of the duplex template. Almost all of the mutant MTF1s support levels of runoff and abortive transcripts like that seen with the WT MTF1. At 0.4 μM the S230C and R264C mutants both show reduced activity (lanes 8 and 12) but at 0.8 μM the levels of transcription are similar to that seen with the WT MTF1 (lanes 9 and 13). **(J-M)** MTF1 enhances promoter specificity and interacts with the unwound NT strand. EMSA experiments were carried out with 14s promoters in which the 5'-end of one of the strands was fluorescently labeled (indicated by an asterisk in the promoters illustrated in panels A-D) and containing a heteroduplex from -4 to +2 (pre-melted promoters; changes in sequence from consensus are indicated by "x-x-x" on the promoter structures). Fluorescent promoter, MtRNAP, and MTF1 concentrations were 1, 0.5, and 0.25 μM, respectively. MTF1 was added at half the mtRNAP concentration and native gels allow resolution of the binary (promoter:MtRNAP) and ternary (promoter:MtRNAP:MTF1) complexes from each other. Unlabeled competitors DNAs of varying structure were then added in varying amounts to determine how promoter structure and sequence affected competition for MtRNAP and MTF1. *Panel J:* The competitor was identical to the labeled promoter and effectively competes for both the ternary and binary complexes. *Panel K:* The competitor is identical in size and has a heteroduplex bubble like the labeled promoter, but the sequence in the promoter region has been changed. This non-promoter competitor competes less effectively for the binary complex and, in particular, competes much less effectively for the ternary complex, consistent with MTF1 increasing the specificity of the IC for promoter DNA. *Panel L:* The competitor is identical to the labeled promoter except that the NT strand from -4 to +2 is missing. The gapped competitor is seen to compete much less effectively for the ternary complex than for the binary complex, indicating that MTF1 binds preferentially to MtRNAP:promoter complexes in which the -4 to +2 region of the NT strand is present. *Panel M:* As in panel L, but using a labeled promoter in which the heteroduplex is generated by changing the consensus sequence of the T-strand rather than NT-strand. The effects of the gapped competitor are similar to panel L, indicating that MTF1 interactions with the -4 to +2 region of the NT-strand are not sequence specific.

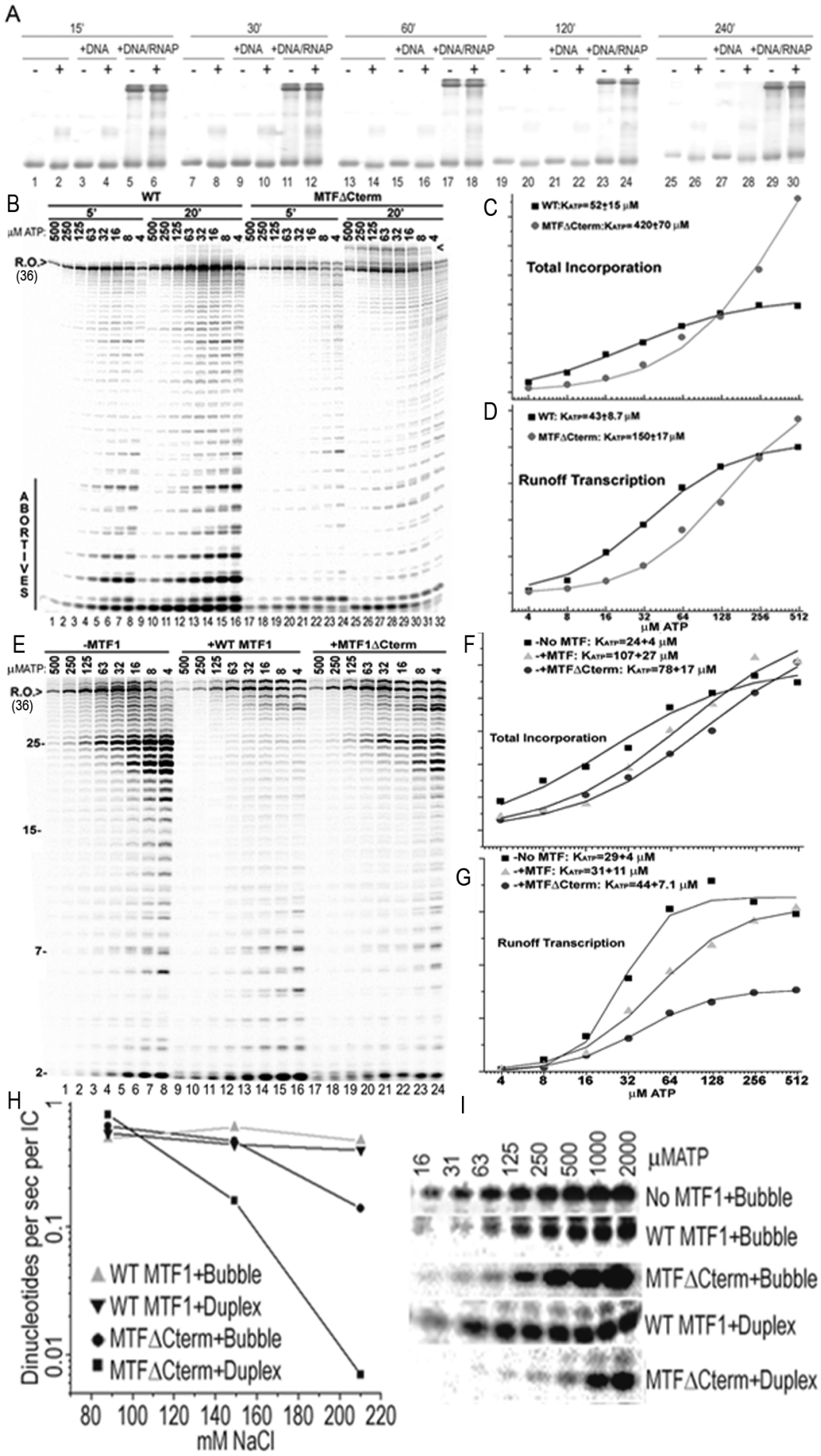

Figure S5 (related to Figure 4 and Table 1). Binding of MTF1 in the IC results in protection of its disordered C-terminal tail, which stabilizes the IC and plays a role in transcription initiation by

affecting the apparent K_{ATP} and K_{NTP} on duplex, but not bubble, promoters. (A) Limiting amounts of carboxypeptidase Y added to MTF1 alone (lanes 2, 8, 14, 20, 26) or MTF1+pre-melted promoter DNA (lanes 4, 10, 16, 22, 28; +DNA= added DNA) results in rapid removal of 8 residues from the MTF1 C-terminus as seen by the shift in migration at the earliest time points (15'; +=carboxypeptidase added; -=no carboxypeptidase; # of residues removed from MTF1 were determined by mass spec). However, the presence of MtRNAP and DNA (lanes 5, 6, 11, 12, 17, 18, 23, 24, 29, 30; +DNA/MtRNAP= added DNA and MtRNAP) protects the MTF1 C-terminus from digestion and no migration shift is seen in reactions with IC even after 240' digestion. **(B-G)** Deletion of MTF1 C-terminal tail increases apparent K_{ATP} for initiation on duplex, but not bubble, promoters. (**B**) Transcripts produced from a 14s duplex promoter in reactions using either WT MTF1 (lanes 1-16) or MTF1 from which residues 324-342 were deleted (lanes 17-32). GTP, CTP, and UTP concentrations in the reactions were 0.5 mM, but [ATP] varied from 500 to 4 μM in serial 2-fold dilutions in lanes 1-8, 9-16, 17-24, and 25-32. The amount of ^{33}P-ATP was constant in all reactions so that the specific activity of the label increases in proportion to the decrease in non-radioactive ATP. Five (lanes 1-8, 17-24) and twenty (lanes 9-16, 25-32) minute reaction time points are shown and abortive and runoff transcripts are labeled. **(C)** Plot of incorporation of ^{32}P into all transcripts ("total incorporation") as a function of [ATP] in reactions with duplex promoters and WT MTF1 (black filled squares) and MTF1ΔCterm (dark grey circles) fit with a Hill equation. **(D)** As in (C) but for incorporation into runoff transcripts ($\geq$36mers) only. (**E**) Transcripts produced from a 14s bubble promoter in reactions with either no MTF1 (lanes 1-8), WT MTF1 (lanes 9-16), or MTF1 from which residues 324-342 were deleted (lanes 17-24). NTP and ^{33}P-ATP concentrations and specific activity as in panel A. The 5 minute reaction point is shown. **(F)** Plot of incorporation of ^{32}P into all transcripts ("total incorporation") as a function of [ATP] in reactions with bubble promoters and No MTF1 (black filled squares), +WT MTF1 (light grey triangles) or MTF1ΔCterm (dark grey circles) fit with a Hill equation. **(G)** As in (F) but for incorporation into runoff transcripts ($\geq$36mers) only. **(H, I)** Deletion of the MTF1 C-terminus increases the salt-sensitivity and apparent K_{NTP} for initiation from duplex, but not pre-melted, promoters. **(H)***:* Rates of dinucleotide synthesis on either bubble or duplex promoters with either WT MTF1 or MTFΔCterm plotted as a function of NaCl concentration. (**I**) Levels of dinucleotide synthesis as a function of varying ATP concentration on pre-melted and duplex promoters and in the presence or absence of WT MTF or MTFΔCterm.

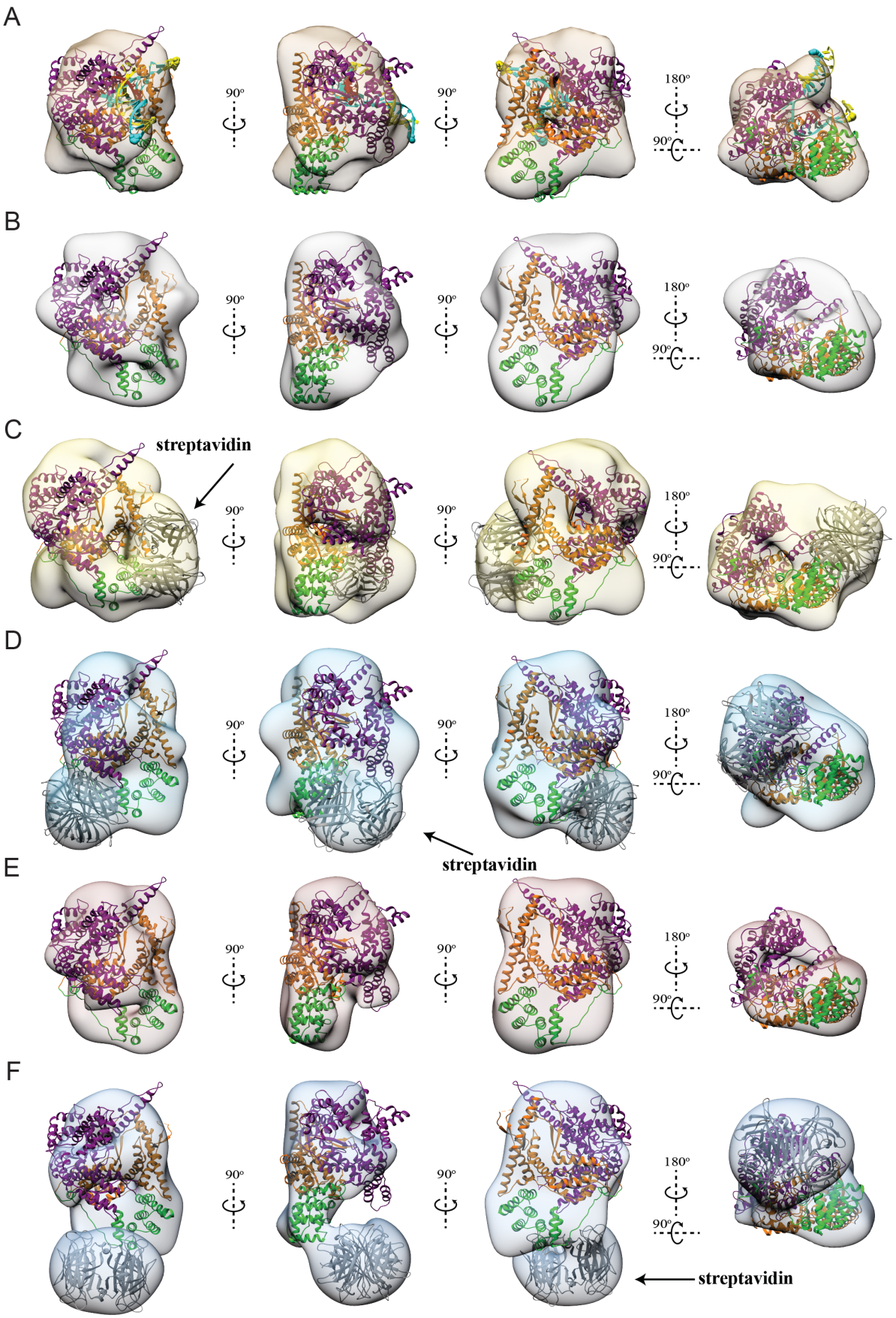

Figure S6 (related to Figures 5 and 6). 3D reconstructions of the ECs. The same views of the 3D reconstructions (together with the docking of the atomic structure of human MtRNAPEC (pdb 4BOC), with DNA not shown except for cryo-EM volume, where the length DNA has been adjusted according to Figure 5: **(A)** EC from unstained, frozen-hydrated particles (9538 particles; 19 Å resolution). **(B)** EC from negatively-stained particles (20873 particles; 19 Å resolution). **(C)** EC in which the 5'-end of the NT-strand DNA is labeled with biotin/streptavidin ('downstream streptavidin EC') (19886 particles; 19 Å resolution). **(D)** EC in which the 5'-end of the T-strand DNA is labeled with biotin/streptavidin ('upstream streptavidin EC') (13240 particles; 19 Å resolution). **(E)** 3D reconstruction of EC assembled with an MtRNAP from which residues 1-241 have been removed (spRNAPIV EC) (17258 particles; 20 Å resolution). **(F)** 3D reconstruction of spRNAPIV EC in which the 5'-end of the NT-strand DNA is labeled with

biotin/streptavidin ('downstream spRNAPIV') (23848 particles; 21 Å resolution).

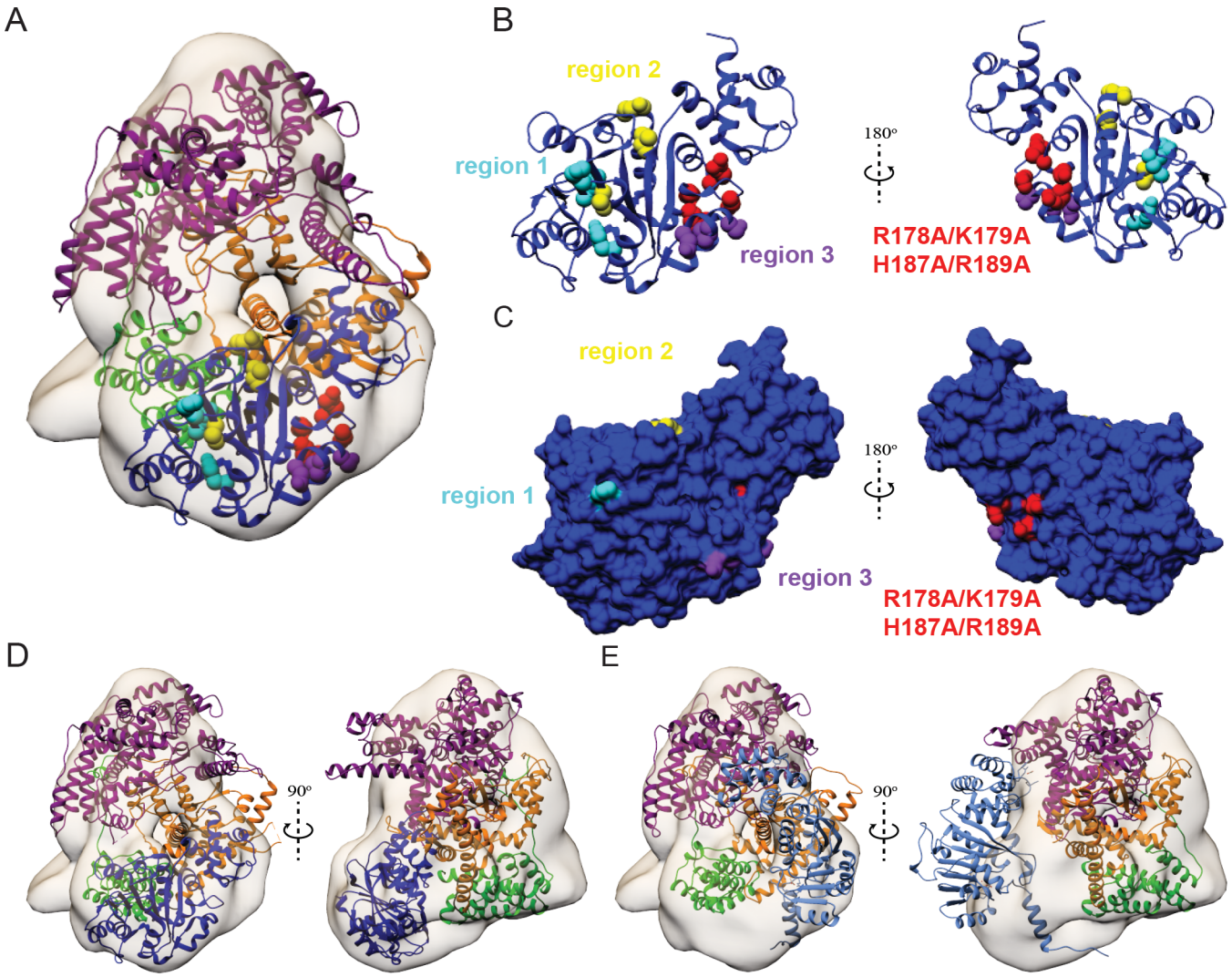

Figure S7. Evaluation of information gathered by biochemical and biophysical approaches with the structural data presented in this study. (**A**) Cryo-EM structure of IC presented together with the docked atomic structures of MtRNAPEC (pdb 4BOC) and MTF1 (pdb 1I4W). Previously reported point mutations (3,4) grouped in three clusters: region 1 (Y42C, H44P and L53H), region 2 (V135A, L154T and K157E) and region 3 (S218R, I221K, D225G) are represented with spheres dyed in cyan, yellow and magenta, respectively. Mutations R178A/K179A and H187A/R189A, placed in positively charged cleft and that were seen to result in the absence of transcription, are represented by red spheres. (**B**) Atomic structure of MTF1 shown as in a (left) and rotated for 180° (right). (**C**) surface generated upon the atomic structure of MTF1 shown as in b and c. (**D and E**) A comparison of the organization of yeast MtRNAP IC presented in this study (D) with that of human MtRNAP IC presented in (5) (E), which reveals the different localization of the two transcription factors. The atomic structure of human MtRNAP (pdb 3SPA) was aligned with the atomic structure of docked human MtRNAPEC (pdb 4BOC), maintaining the relative position towards the atomic structure of human MTFB (pdb 4GC5),atomic structure dyed in light blue in (E).

Supplemental references

1. Biswas, T.K., Ticho, B. and Getz, G.S. (1987) In vitro characterization of the yeast mitochondrial promoter using single-base substitution mutants. *J Biol Chem*, **262**, 13690-13696.
2. Greiner, D.P., Miyake, R., Moran, J.K., Jones, A.D., Negishi, T., Ishihama, A. and Meares, C.F. (1997) Synthesis of the protein cutting reagent iron (S)-1-(p-bromoacetamidobenzyl)ethylenediaminetetraacetate and conjugation to cysteine side chains. *Bioconjug Chem*, **8**, 44-48.
3. Shadel, G.S. and Clayton, D.A. (1995) A Saccharomyces cerevisiae mitochondrial transcription factor, sc-mtTFB, shares features with sigma factors but is functionally distinct. *Molecular and cellular biology*, **15**, 2101-2108.
4. Cliften, P.F., Park, J.Y., Davis, B.P., Jang, S.H. and Jaehning, J.A. (1997) Identification of three regions essential for interaction between a sigma-like factor and core RNA polymerase. *Genes & development*, **11**, 2897-2909.
5. Yakubovskaya, E., Guja, K.E., Eng, E.T., Choi, W.S., Mejia, E., Beglov, D., Lukin, M., Kozakov, D. and Garcia-Diaz, M. (2014) Organization of the human mitochondrial transcription initiation complex. *Nucleic acids research*, **42**, 4100-4112.